Supplementary Figure 1

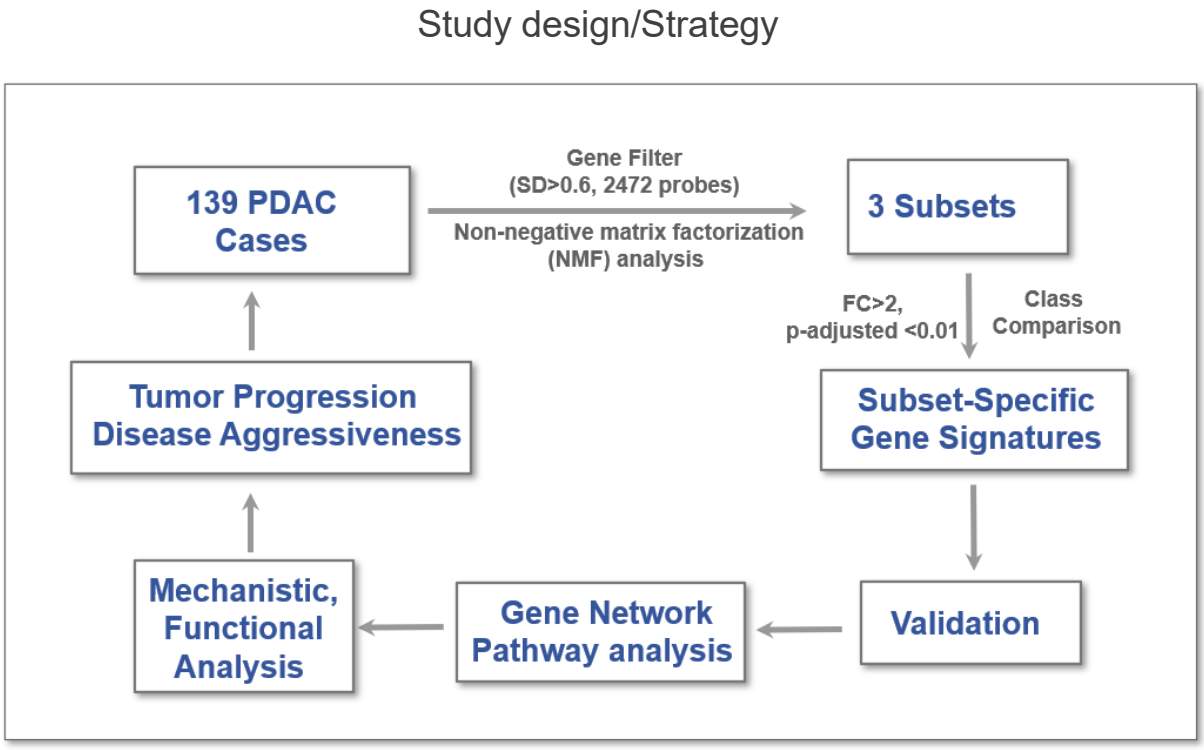

Schematic representation of the strategy used in the study to investigate the underlying mechanisms of disease aggressiveness in PDAC patients.

Supplementary Figure 2

A

Publicly available datasets for validation Cohort

Cohort	Number of Cases	Publication
GSE16515 (Pei Cohort)	37	Hepatogastroenterology, 2008
GSE15471 (Badea Cohort)	39	Cancer Cell, 2009
TCGA	176	

B

Badea Cohort (GSE15471)

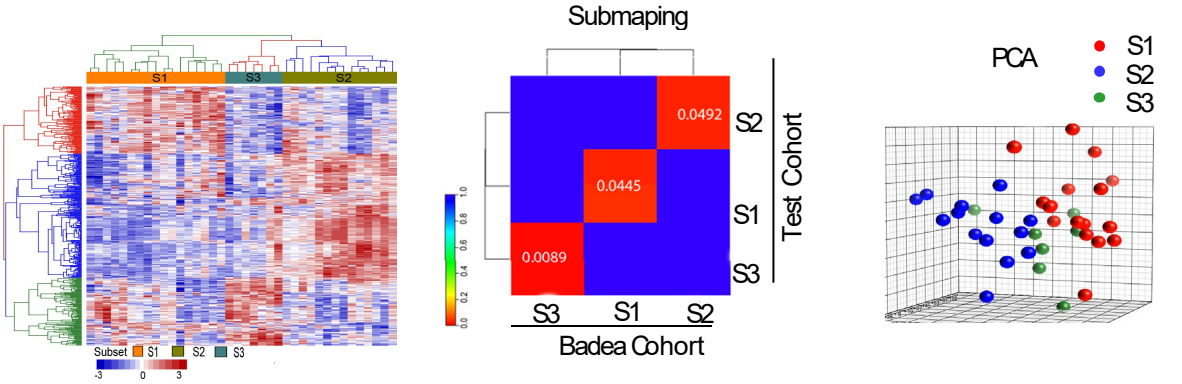

C

Pei Cohort (GSE16515)

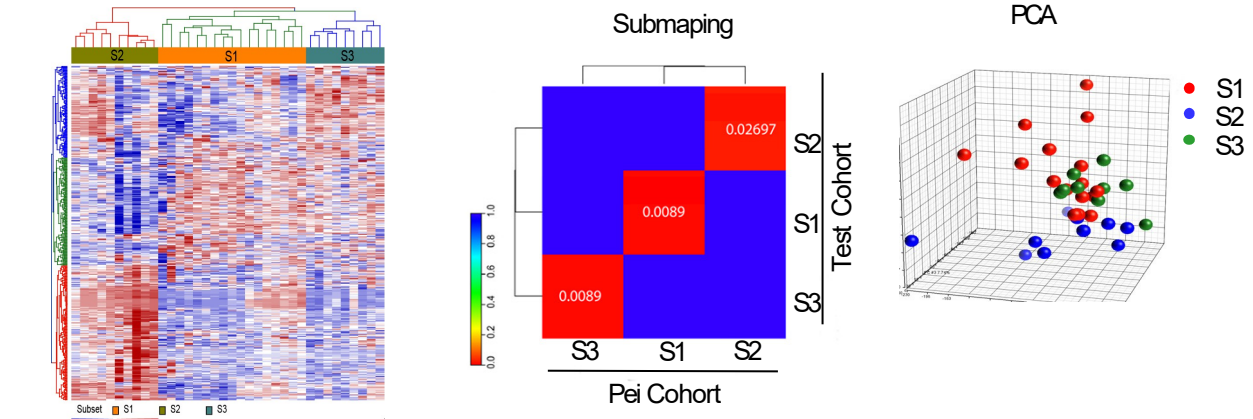

D

TCGA

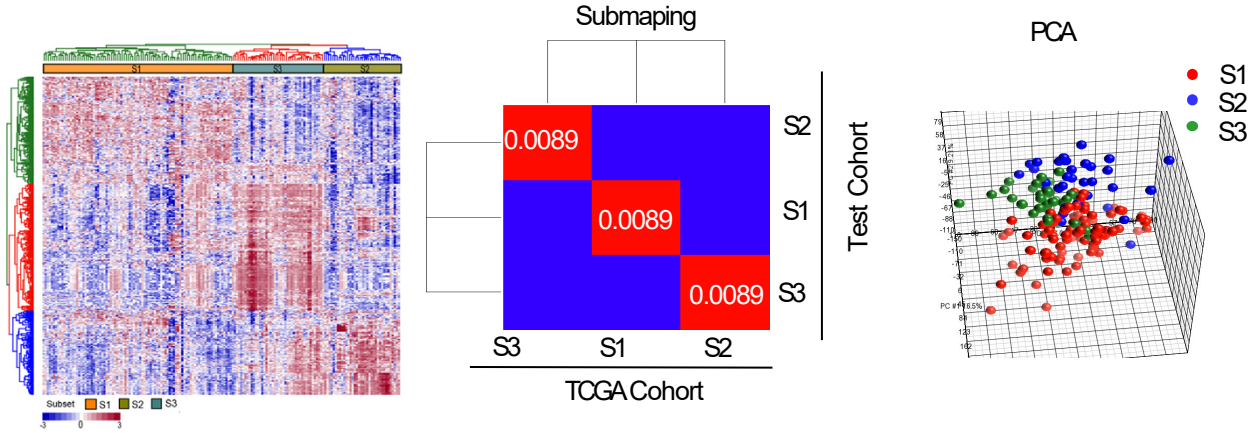

Supplementary Figure 2. Validation of PDAC subsets in publicly available datasets. **A**, Brief summary of the publicly available dataset used in the study for validation; **B**-**D**, Validation of molecular subsets using our molecular signature by unsupervised hierarchical clustering analysis. Heat map showing three subsets of PDAC in Badea cohort (GSE15471), Pei Cohort (GSE16515) and TCGA cohort (Left panel); Middle panels showing subclass mapping of subsets in our cohort and the other three datasets. Statistically significant associations between subsets are represented by Bonferroni-adjusted *P* values. Significant associations showing similarity between subsets are shown in red, with $P < 0.05$, while differences between subsets (Bonferroni-adjusted $P = 1$) are shown in blue. Right panel: Principal component analysis showing three molecular subsets in Badea cohort (B), Pei Cohort (C) and TCGA cohort (D) as defined by our gene signature.

Supplementary Figure 3

Comparison of subsets (S1, S2, S3) as defined in our study with Moffitt cohort (classical and basal-like) (7) and Collisson cohort (5) (classical, quasi-mesenchymal and exocrine-like).

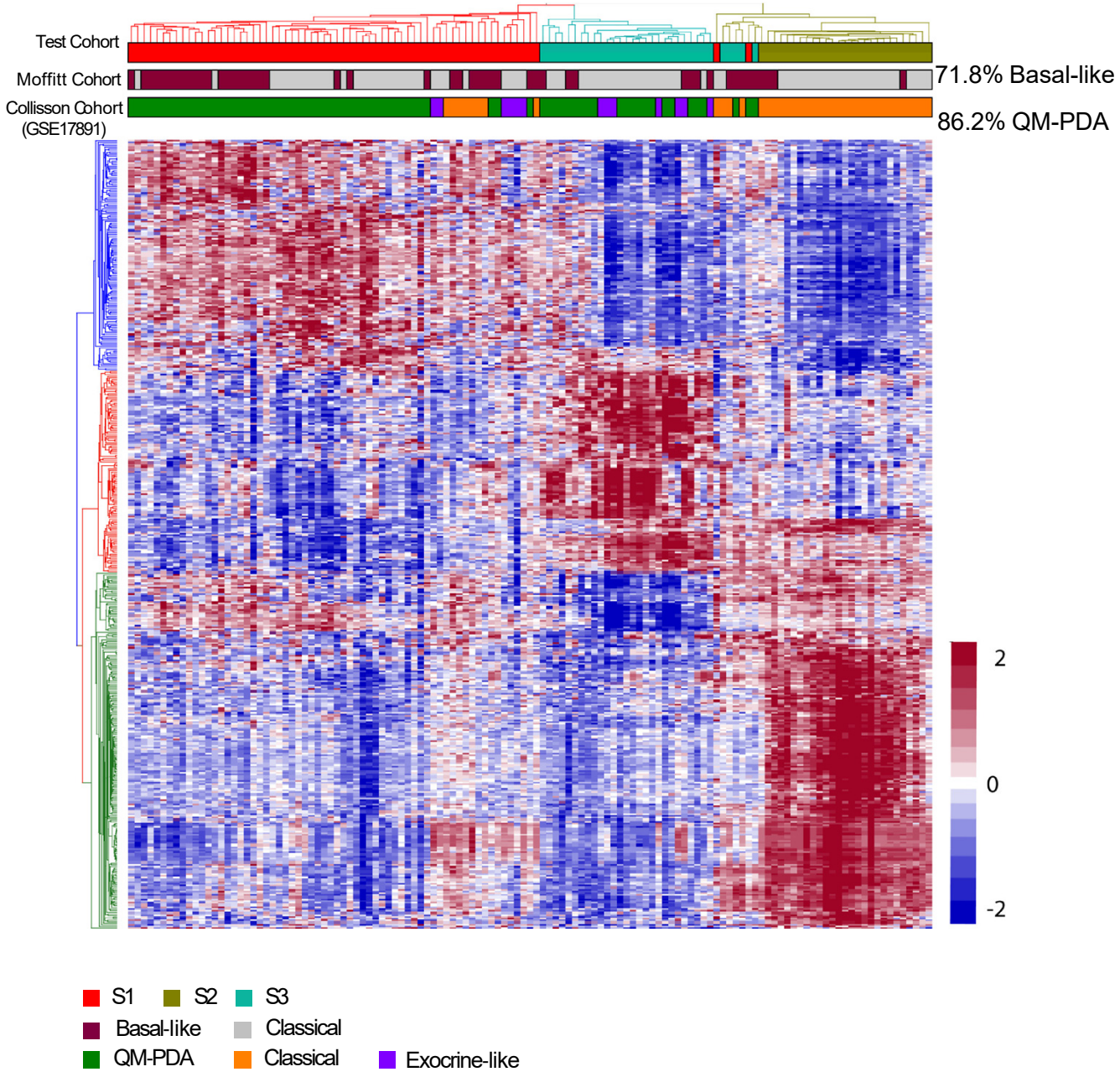

Comparison of subsets (S1, S2, S3) as defined in our study with Moffitt cohort (classical and basal-like) (7) and Collisson cohort (5) (classical, quasi-mesenchymal and exocrine-like). We performed unsupervised hierarchical clustering analysis in our cohort by using subtype specific gene signature from Moffit cohort and Collisson cohort. This led to the identification of their defined molecular subtypes in our cohort. Percentage indicates the overlap of basal-like or quasi-mesenchymal subtype with our subset-1 patients.

Supplementary Figure 4

Identification of cell line representing molecular subset using gene expression data from Cancer Cell Line Encyclopedia (CCLE), (Ref 19).

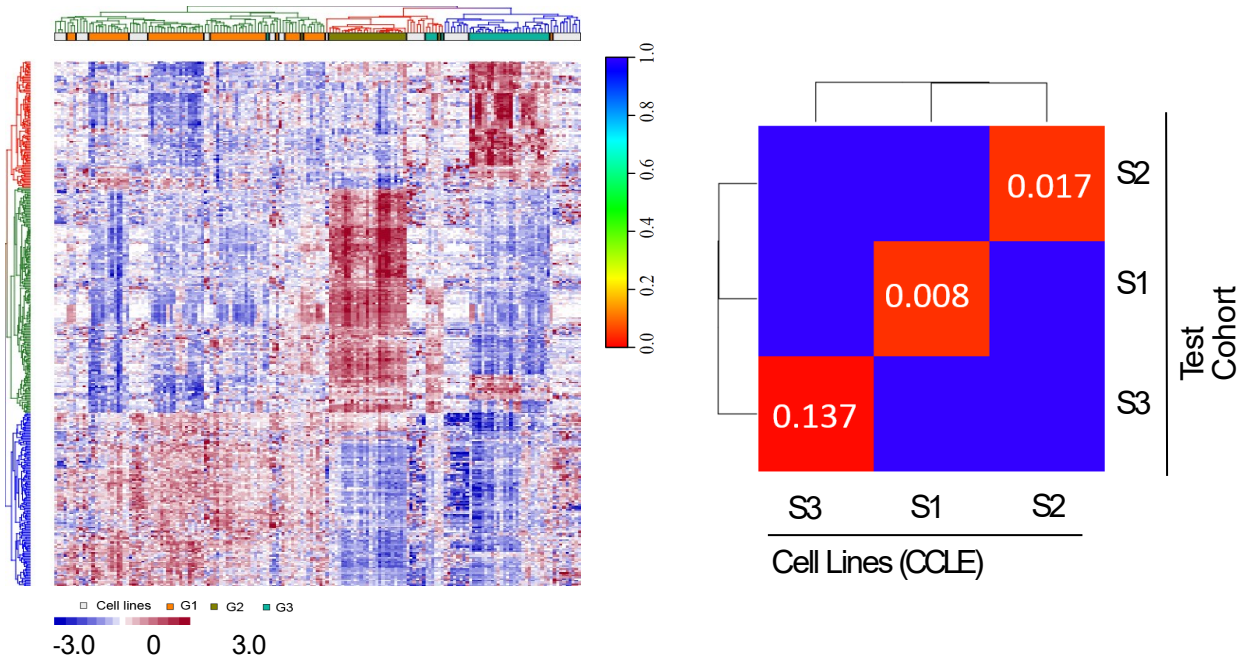

Identification of pancreatic cancer cell lines which represents different subsets among our patients' cohort by using gene expression datasets from Cancer Cell Line Encyclopedia (CCLE). Heat map showing three subsets in distance weighted discrimination (DWD) - test cohort and dataset from CCLE (Left panel). Similarity between subsets was analyzed by subclass mapping (Right Panel). $P < 0.05$ showed significant association between subsets.

Supplementary Figure 5

Knockdown of Clusterin significantly enhanced proliferation, colony formation, migration and invasion in pancreatic cancer

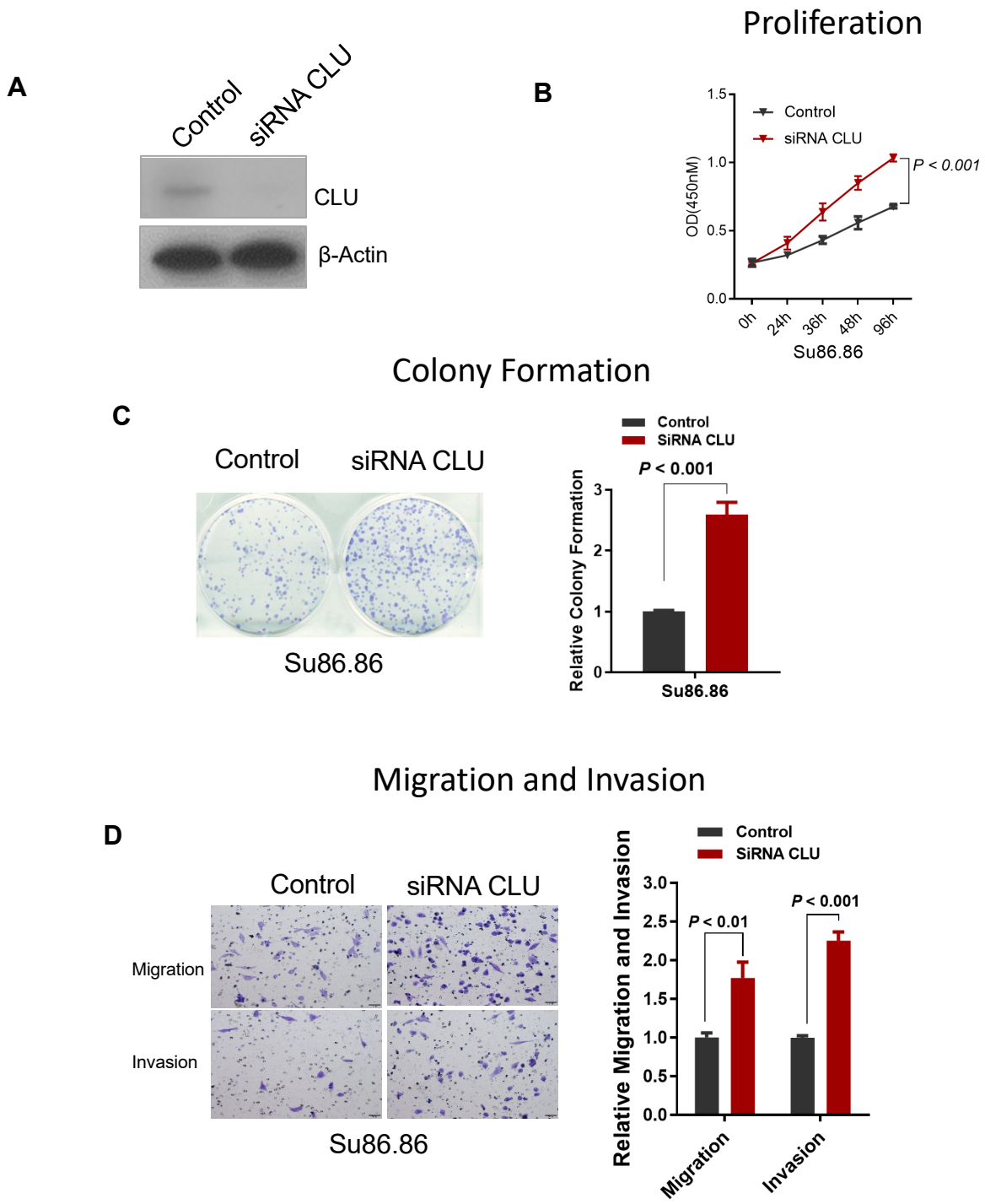

Knockdown of Clusterin significantly enhanced proliferation, colony formation, migration and invasion. **A**, Knockdown CLU expression as determined by immunoblotting. **B**, CLU-knockdown resulted in a marked increase of proliferation in Su86.86 cells. **C**, CLU-knockdown cells showed enhanced colony formation as compared with control cells. **D**, CLU-knockdown significantly enhances migration and invasion in Su86.86 cells.

Supplementary Figure 6

CLU accumulated in the nuclei and induced apoptosis in pancreatic cancer cell lines representing subset-1

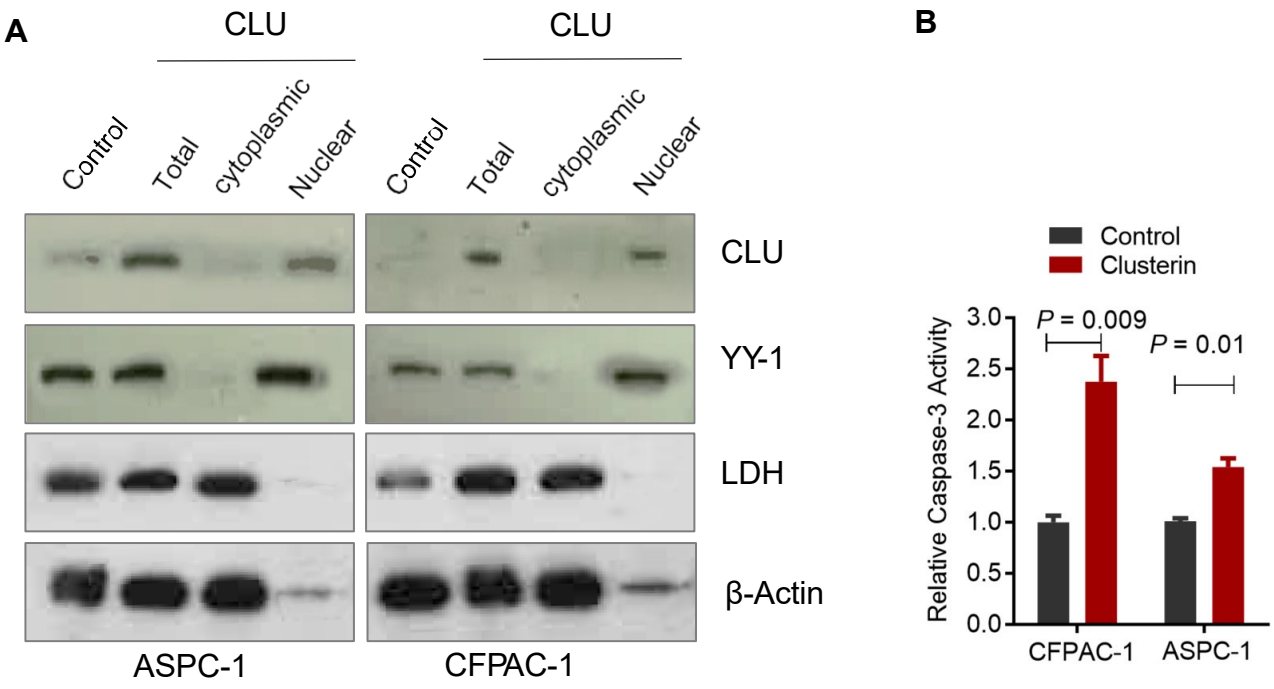

CLU accumulated in the nuclei and induced apoptosis in pancreatic cancer cell lines representing subset-1. **A**, Immunoblotting of subcellular fractions of CLU in pancreatic cancer cell lines, ASPC-1 and CFPAC-1 representing subset-1. The purity of each fraction was verified using antibodies against YY-1 for nuclear and LDH for cytoplasmic fractions, respectively. **B**, Overexpression of CLU led to a significant increase in caspase-3/7 activity in CFPAC-1 and ASPC-1.

Supplementary Figure 7

Immunohistochemical staining of CLU in PDAC patients

A

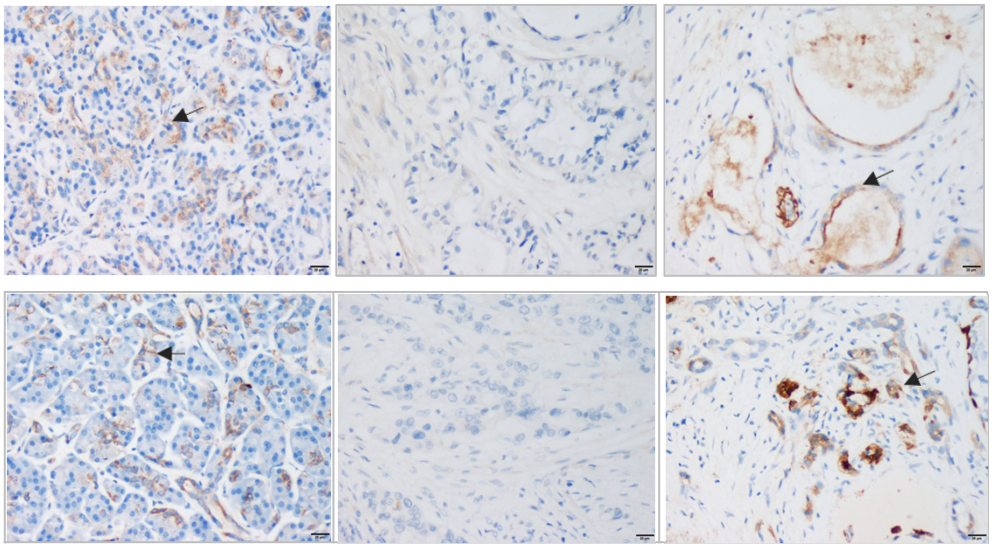

B

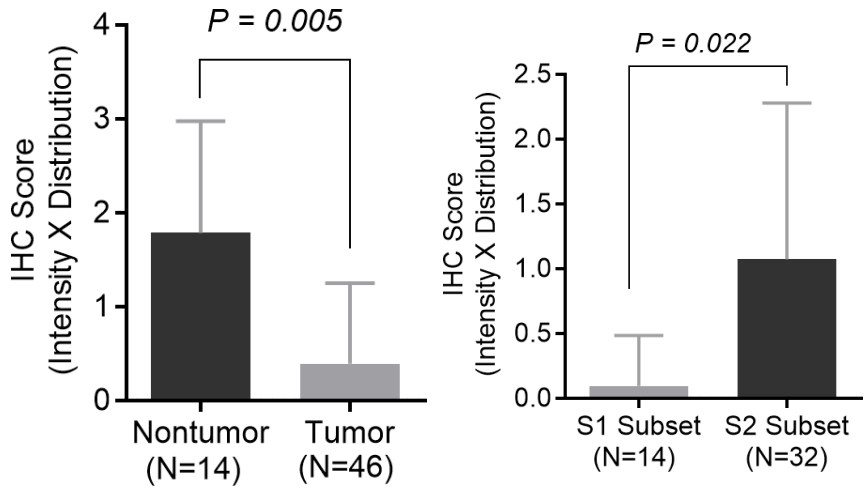

Immunohistochemical staining of CLU in PDAC patients. A lower expression of CLU was found in tumors as compared to nontumor tissues from PDAC patients, and tumors representing subset-1 showed a reduced expression of CLU as compared with tumors from subset 2 patients. **A**, Representative images of CLU staining in nontumor and tumor representing subset-1 and subset-2 patients. **B,** Quantitation of imunohistochemical staining of CLU was performed by multiplying the intensity and prevalence scores as described earlier (47).

Supplementary Figure 8

CLU negatively correlates with miR-21 in tumors from PDAC patients

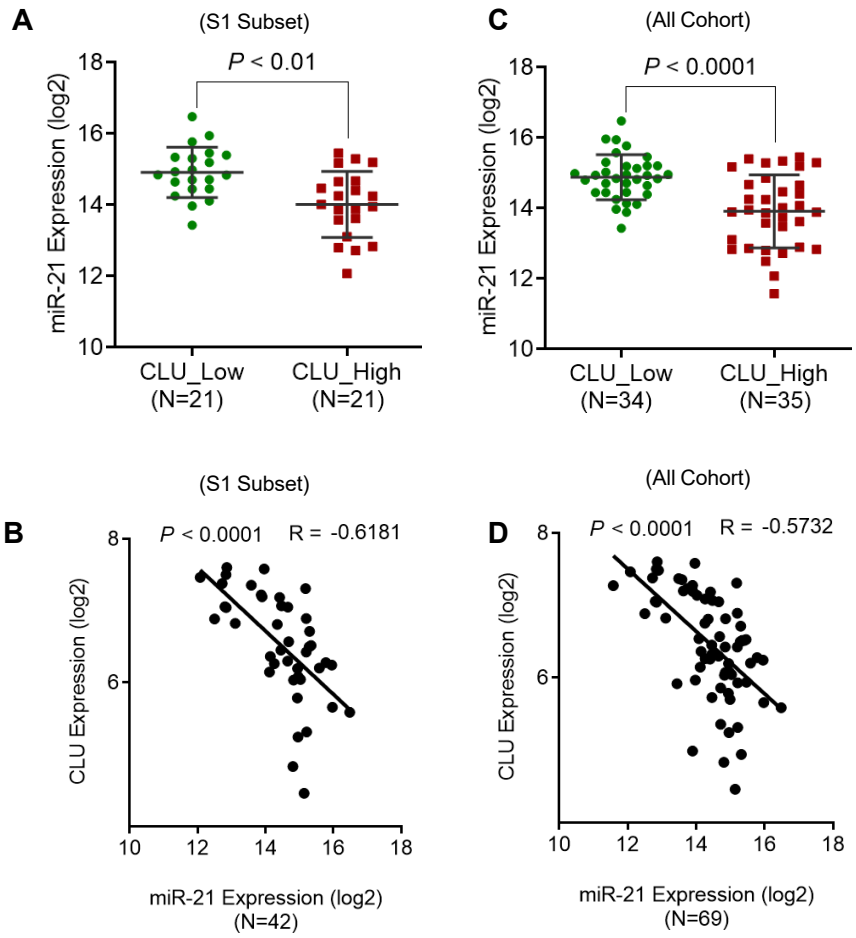

CLU negatively correlates with miR-21 in tumors from PDAC patients. A-D, Tumors with a lower CLU expression shows a higher level of miR-21 as compared to tumors with high CLU expression and a negative correlation existed between CLU and miR-21 gene expression in subset 1 as well as in all the patients combined in the test cohort.